Vol 16 No 3, March 2007
1009-1963/2007/16(03)/0843-05
Chinese Physics
© 2007 Chin. Phys. Soc.
and IOP Publishing Ltd

Electron emission degradation of nano-structured sp^2-bonded amorphous carbon films*

Lu Zhan-Ling(鲁占灵)[a)b)], Wang Chang-Qing(王昶清)[a)], Jia Yu(贾 瑜)[a)], Zhang Bing-Lin(张兵临)[a)†], and Yao Ning(姚 宁)[a)]

[a)] *Key Laboratory of Material Physics of Education Ministry of China, Department of Physics, Zhengzhou University, Zhengzhou* 450052, *China*

[b)] *Department of Material Science and Engineering, Zhengzhou University, Zhengzhou* 450052, *China*

(Received 25 October 2005; revised manuscript received 25 September 2006)

The initial field electron emission degradation behaviour of original nano-structured sp^2-bonded amorphous carbon films has been observed, which can be attributed to the increase of the work function of the film in the field emission process analysed using a Fowler–Nordheim plot. The possible reason for the change of work function is suggested to be the desorption of hydrogen from the original hydrogen termination film surface due to field emission current-induced local heating.

For the explanation of the emission degradation behaviour of the nano-structured sp^2-bonded amorphous carbon film, a cluster model with a series of graphite (0001) basal surfaces has been presented, and the theoretical calculations have been performed to investigate work functions of graphite (0001) surfaces with different hydrogen atom and ion chemisorption sites by using first principles method based on density functional theory-local density approximation.

Keywords: nano-structured sp^2-bonded amorphous carbon film, field emission, work function
PACC: 7970, 7360N, 7115A

1. Introduction

Hydrogenated amorphous carbon (a-C:H) film is a complex disordered form of carbon which exhibits an amazing diversity of properties, depending on the preparation method and the deposition conditions.[1] So it has attracted considerable interest during the last two decades because of its potential applications in quite different domains.[1−5] One of the most outstanding applications is the production of thin-film field-emission cathodes for vacuum micro-electronics. Before this novel material can be made ready for commercial use, stability of the devices under different field-emission conditions must be considered. Many factors such as ion bombardment, adsorption and desorption of residual gas molecules, cathode heating-up, etc., separately or in combination, result in a number of effects changing the performance of the field-emission cathode (FEC). It has been found empirically that electrode conditioning (repeated discharge, aging) is helpful to improve the stability of carbon-based FEC, such as diamond-like carbon film, carbon nanotube and carbon fibre.[6−9] On the other hand, the emission characteristics of unconditioned surfaces (original surface state) are known to be unstable.[10] But the origins for such instability are still unclear. Knowledge of the emission behaviour in the original surface state is valuable for not only the design of electronic devices but also understanding of interrelation of carbon materials structure with their emission properties.

In this paper we present the experimental results of the initial electron emission degradation behaviour of original nano-structured sp^2-bonded amorphous carbon film, and theoretical calculation has been performed to confirm the experimental conclusion.

2. Experiment

The nano-structured sp^2-bonded amorphous carbon film composed of carbon particles with sizes of about 20 nm is deposited on titanium-coated ceramic substrate by microwave plasma chemical vapour deposition (CVD). The deposition conditions

*Project supported by the Science and Technology Foundation of Education Ministry of China (Grant No 205091).
†Corresponding author. E-mail: blzhang@zzu.edu.cn

and the structure of the films have been reported previously.[11] The field electron (FE) emission characteristic of the film is measured by diode structure in a vacuum chamber of below 5×10^{-5} Pa. The distance between the sample cathode and the anode is about 270 μm. The voltage is stepped up and down from 0 to 1000 V for several cycles until the stable emission is obtained.

The field emission characteristics of the film are shown in Fig.1. During field emission measurements the turn-on field (current density of 1 μA/cm^2) of 0.74 V/μm is obtained for the first run. In the second run the turn-on field increases and the field emission current of the film is obviously degraded. After several voltage cycles the turn-on field gradually stabilizes at 2.0 V/μm and the current density of 0.70 mA/cm^2 at an electric field of 3.70 V/μm is kept, and the I–V curves become reproducible. The Fowler–Nordheim (F–N) plots of the first and fifth runs shown in Fig.2 are almost straight lines, showing that the mechanism of the electron emission from the materials is linked to field emission by the tunnel effect.

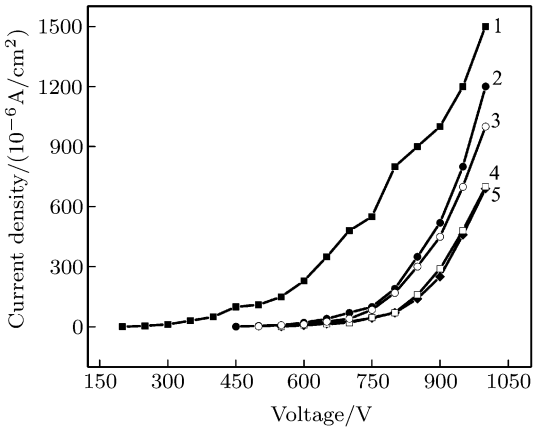


Fig.1. I–V curves of the film.

What is the reason of the degradation observed in the initial field emission stage? The slope of F–N plot of the first run is seen to be lower than that of the fifth run as shown in Fig.2. According to F–N theory, the slope of the F–N plot is given by

$$b = -6.83 \times 10^9 \phi^{3/2} d/\beta, \qquad (1)$$

where b is the slope of the F–N plot, ϕ is the work function of the film, d is the inter electrode distance, β is field enhancement factor determined by geometrical shape of the film, which is not changed obviously as observed by scanning electron microscopy. The increase of the slope of the F–N plot means the increase of the work function of the film. It is known that the surface of all kinds of carbon-based films grown by CVD methods are terminated by hydrogen, which will be desorbed from the original film surface due to field-emission current-induced local heating. It has been observed in experiments that chemisorptions of hydrogen on sp^2-bonded carbon lead to a lowering of the electron work function,[12] so the desorption of hydrogen may result in the increase of surface work function of the film and then increase the barrier to field emission.

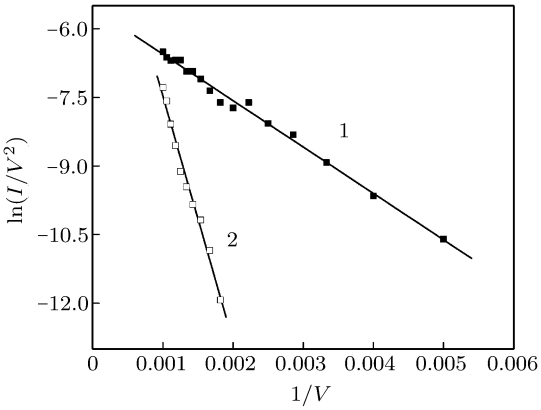


Fig.2. F–N plots 1 and 2 corresponding to curves 1 and 5 in Fig.1 respectively.

In order to examine the above suggestion, theoretical calculations have been used to explain the experimental phenomena as an approximation in the next section.

3. Theoretical calculations

The diamond films also show better field emission characteristics due to the hydrogen termination.[13] The electronic structure of diamond surfaces has been calculated[14–17] and the results show that the hydrogen termination can reduce the energy barrier for electron emission by lowering the electron affinity of diamond surface.

Although chemisorption of hydrogen on sp^2-bonded carbon surfaces, including C_{60} multilayer films, single-walled carbon nanotubes, and graphite (0001), lead to a lowering of the work function observed by experiment,[12] and chemisorption properties of H atom on graphite surface have been theoretically investigated by many authors,[18–23] up to now the accurate theoretical calculation of the change of work function of sp^2-bonded carbon surfaces due to hydrogen chemisorptions has not been reported. In

this paper we investigate the work function change of hydrogen-adsorbed sp^2-bonded amorphous carbon surfaces by using first principles method based on density functional theory-local density approximation (DFT–LDA). For simplicity, a cluster model is presented, which suggests that the nano-structured amorphous carbon grain consists of a series of graphite (0001) basal surface clusters, then the theoretical calculations are performed to investigate work functions of graphite (0001) surfaces with different hydrogen atom and ion chemisorption sites by using first principles method based on DFT–LDA.

3.1. Model and calculation methods

An asymmetric supercell approach with periodic boundaries has been employed to model graphite (0 0 0 1) surface. The substrate consists of five carbon layers with (2×2) surface cells that contain eight carbon atoms per layer. A vacuum space of 12 Å has been used to separate the graphite substrate and its repeatable images. In the structure optimization process, the carbon atoms in the bottom two layers are kept fixed at their bulk-like positions, only the carbon atoms in the upper three layers and the hydrogen atom (H) are allowed to move in all directions.

The first-principle calculations presented in this paper have been performed using *ab initio* total-energy code Vienna *ab initio* simulation package. The approach in the code is based on DFT calculations. The exchange–correlation function is considered in the form of LDA. The interactions between the ionic cores and the electrons are described by projector augmented wave scheme. Monkhorst–Pack special K points are used in integrating the periodic functions of Bloch wave vector over the Brillouin zone of the sample. The plane wave cut-off energy is set to be 400 eV. The optimization is terminated when the change of the total energy is less than 0.001 eV.

3.2. Hydrogen atom adsorption on graphite (0001) surface

Firstly we optimize the clean graphite performed via either a conjugate gradient or a quasi-Newton minimization. The same optimized lattice constants of $a_0 = 2.453$ Å and $c_0 = 6.647$ Å are obtained by using the two methods, which are in agreement with the experimental values $a_0 = 2.456$ Å and $c_0 = 6.696$ Å.[24]

Then we put one H at an initial distance of 1.5 Å above the surface in each (2×2) graphite surface supercell and let the system relax. The H coverage is thus 1/8 of a monolayer in the present paper. Four high-symmetry sites on the graphite (0 0 0 1) surface have been examined with respect to H binding: the bridge between two nearest-neighbour carbon atoms (BR), the hollow of the hexagonal ring (HL), and the two nonequivalent top sites of a surface carbon, one type has a carbon atom directly below it (T_1), and the other does not (T_2).

The relaxed structure parameters and adsorption energies are shown in Table 1. The results show that the equilibrium C–H bond lengths are 1.14, 1.14, 1.35, 2.21 Å and the adsorption energies of 1.883, 1.904, 1.208, 0.402 eV for H atom above T_1, T_2, BR, HL sites respectively. The position of the C atom bonded to H atom is pulled out of the basal plane by $\Delta h = 0.30$ Å for two top sites which give rise to a local sp^3-like hybridization as shown in Fig.3, while for H atom above the BR and HL sites only negligible surface reconstruction is observed.

Table 1. Relaxed structure parameters and binding energy of H atom adsorbed on graphite surface.

H bonding sites	adsorption energy /eV	C–H bond length/Å	Δh/Å
T_1	1.883	1.14	0.30
T_2	1.904	1.14	0.30
BR	1.208	1.35	0.05
HL	0.402	2.21	0.02

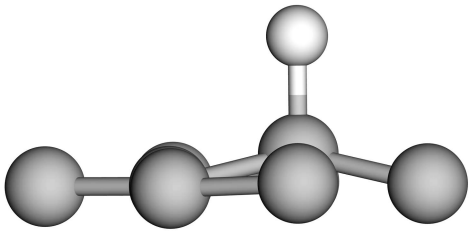


Fig.3. Relaxed structure of graphite (0001) surface for H adsorbed on T_1 site. The C atom is pulled above the graphite plane.

The charge density plots corresponding to H adsorption above the four sites are shown in Fig.4. The plane of the plots corresponds to a z-axis slice through the supercell. The charge density distribution reveals that the charge transfers between the H and the surface for H above T_1, T_2 and BR sites, indicating that

the binding is of chemical nature. However, no significant electron transfer occurs between the H atom and the surface for H above HL site, and thus the adsorption is of physical nature. A detailed analysis of the C–H bond lengths and the adsorption energies can also indicate that H above T_1, T_2, BR sites are chemisorption and H above HL is physical adsorption. In the following, we only calculate the work function changes of graphite (0001) surface due to H atom and hydrogen ion adsorbed on T_1, T_2 and BR sites.

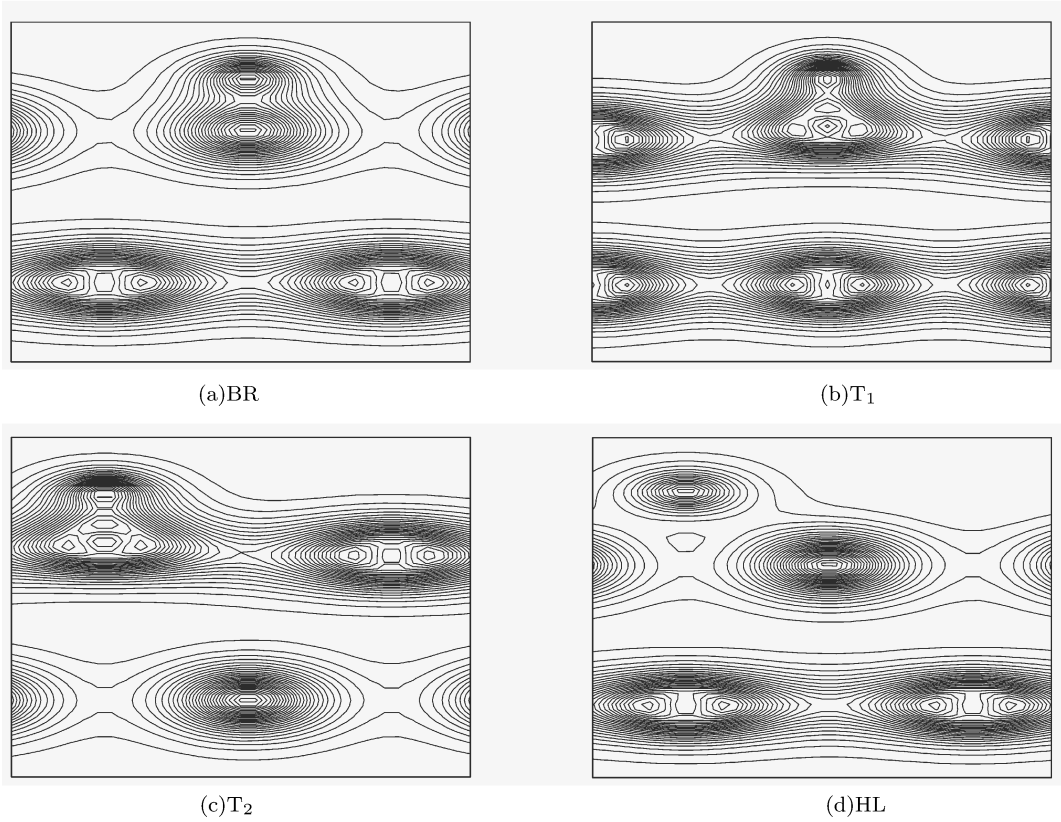


Fig.4. The charge density plots corresponding to H adsorption above the four sites of (a) BR, (b) T_1, (c) T_2 and (d) HL. The plane of the plots corresponds to a z-axis slice through the supercell.

3.3. Work functions of graphite (0001) surface

DFT-LDA calculations have been performed to investigate vacuum level and Fermi level, the difference between them is the work function. The calculated work function of clean graphite (0001) surface (ϕ_0) using p(2×2) supercell is 4.652 eV. The work functions (ϕ) of graphite (0001) surface and the work function changes ($\Delta\phi = \phi - \phi_0$) due to H atom chemisorption on its surface are listed in Table 2.

Table 2. Calculated values for graphite (0 0 0 1) surface due to H atom adsorption.

H adsorption sites	ϕ/eV	$\Delta\phi$/eV
BR	3.614	−1.038
T_1	3.725	−0.927
T_2	3.687	−0.965

We also calculate the ϕ and $\Delta\phi$ of graphite (0001) surface due to hydrogen ion chemisorption on its surface since the carbon film surface grown in plasma (CH_4+H_2) will be terminated either by H atom or hydrogen ion. The calculated results are listed in Table 3.

Table 3. Calculated values for graphite (0 0 0 1) surface due to H ion adsorption

H^+ bonding sites	ϕ/eV	$\Delta\phi$/eV
BR	2.539	−2.113
T_1	2.472	−2.180
T_2	2.454	−2.198

The calculated results in Tables 2 and 3 reveal that the work function of graphite (0001) surface is obviously lowered due to H or H^+ chemisorption on

either top sites or bridge site. The values of the lowering of work function due to H and H^+ chemisorption can be up to 1.038 eV and 2.198 eV respectively. It is in agreement with the experimental results that H^+ treatment lowers the work function of sp^2 carbon more than that of H treatment.[12]

The calculated results can explain the experimental phenomena that the origin of the observed initial current degradation and the increasing slope of F–N plot is the desorption of hydrogen from the original hydrogen termination film surface, which results in the increase of the work function of the film and thus substantially increases the barrier to field emission.

4. Conclusions

The experiments indicate that the nano-structured sp^2-bonded amorphous carbon film is an efficient cathode material at low electric field. The initial emission degradation behaviour of the film during the field-emission process can be attributed to the desorption of hydrogen from the original hydrogen termination surface due to field-emission current-induced local heating, which results in the increase of the work function of the film from the analysis of F–N plot. The theoretical results reveal that hydrogen termination on graphite (0001) surface can significantly lower the work function of the film surface, which is in agreement with our experimental results.

References

[1] Robertson J 2002 *Mater. Sci. Eng.* R **37** 129
[2] Hauert R 2003 *Diamond Rel. Mater.* **12** 583
[3] Forbes R G 2001 *Solid-State Electron.* **45** 779
[4] Ferrari A C 2004 *Surf. Coat. Technol.* **180-181** 190
[5] Zhang L, Ma H Z, Li H J, Yang S E, Yao N, Hu H L and Zhang B L 2004 *Acta Phys. Sin.* **53** 883 (in Chinese)
[6] Mousaa M S and Kellyb T F 2003 *Ultramicroscopy* **95** 125
[7] Takahashi E, Ebe A, Oqata K, Komuro S, Mitsui H and Sone M 2001 *Electrical Engineering in Japan* **136** 10
[8] Inomoto H, Hatta A, Kawabata K, Katoda T and Hiraki A 2000 *Diamond Rel. Mater.* **9** 1209
[9] Jiang J, Zhang J H, Feng T, Jiang B Y, Wang Y J, Zhang F M, Dai L J, Wang X, Liu X H and Zou S C 2005 *Solid State Commun.* **135** 390
[10] Geis M W, Twichell J C and Lyszczarz T M 1996 *J. Vac. Sci. Technol.* B **14** 2060.
[11] Lu Z L, Wang C Q, Jia Y, Zhang B L and Yao N 2006 *Vacuum Electronics* (1) 58 (in Chinese)
[12] Ruffieux P, Gröning O and Bielmann M 2004 *Appl. Phys.* A **78** 975
[13] Cui J B, Ristein J, Stammler M, Janischowsky K, Kleber G and Ley L 2000 *Diamond Rel. Mater.* **9** 1143
[14] Furthmüller J, Hafner J and Kresse G 1996 *Phys. Rev.* B **53** 7334
[15] Kern G and Hafner J 1997 *Phys. Rev.* B **56** 4203
[16] Himpsel F J, Knapp J A, Van Vechten J A and Eastmann D E 1979 *Phys. Rev.* B **20** 624
[17] Yu Y, Gu C Z and Xu L F 2004 *Acta Phys. Sin.* **53** 2710 (in Chinese)
[18] Österlund L, Chakarov D V and Kasemo B 1999 *Surface Science* **420** 174
[19] Kanashenko S L, Gorodetsky A E, Chernikov V N, Markin A V, Zakharov A P, Doyle B L and Wampler W R 1996 *J. Nucl. Mater.* **233** 1207
[20] Frenklach M and Wang H 1991 *Phys. Rev.* B **43** 1520
[21] Sha X W and Jackson B 2002 *Surface Science* **496** 318
[22] Jeloaica L and Sidis V 1999 *Chem. Phys. Lett.* **300** 157
[23] Volpe M and Cleri F 2003 *Surface Science* **544** 24
[24] http://cst-www.nrl.navy.mil/lattice/struk.xmol/a9.pos